Journal of Ceramic Processing Research. Vol. 15, No. 1, pp. 53~56 (2014)

J O U R N A L O F
Ceramic Processing Research

Characterization of nano-scale strained silicon-on-insulator substrates by multi-wavelength high resolution micro-raman and optical reflectance

Tae-Hun Shim, Du-Yeong Lee, Tae-Hyun Kim and Jea-Gun Park*
Advanced Semiconductor Materials and Devices Development Center, Hanyang University, Seoul 133-791, Korea

Strained silicon-on-insulator (sSOI) substrates were characterized using multi-wavelength, high resolution, polychromator-based micro Raman spectroscopy and normal incidence optical reflectance spectra measurement. Significant Raman shifts towards the lower wavenumber side, corresponding to tensile stress, and broadening of the Raman peak in sSOI thin films were observed. The stress and crystallinity of sSOI were characterized from the shift and full-width-at-half-maximum data. The thickness of strained Si and buried oxide film of sSOI was estimated from the optical reflectance. Multi-wavelength Raman and optical reflectance measurement, when used together provide a useful and practical non-destructive stress, and structural characterization technique for nano-scale sSOI.

Key words: Strained Si, sSOI, SOI, Multi-wavelength, Raman, Reflectance, Strain.

Introduction

Strain engineering has been a key research area for channel mobility enhancement for over a decade. High mobility of a strained Si channel has been widely used in high performance, complementary metal-oxide-semiconductor field effect transistors (CMOSFETs) [1-3]. For further device performance enhancement, stress and strain engineered Si, SiGe/Si, strained silicon-on-insulator (strained SOI or sSOI) and strained Si grown on a relaxed SiGe-on-insulator (SGOI) have been explored [1-7]. The sSOI configuration is believed to be suitable for 45 nm generation and smaller devices in high speed and broadband communications applications.

Nano-scale strained Si and ultra-thin silicon-on-insulator (SOI) substrates are intended for fully depl eted (FD) device applications to reduce short channel effects in CMOSFET with a design rule of 45 nm generation [8]. Since devices are directly fabricated on SOI or sSOI substrates, the properties of the basic materials must be well characterized and monitored. Non-destructive and easy-to-implement in-line characterization techniques must be developed for commercial applications.

Raman spectroscopy is a non-contact and nondestructive characterization technique which is very sensitive to strain and stress in semiconductor crystals such as Si, Ge, $Si_{1-x}Ge_x$, GaAs, GaN, SiC etc [9-12]. There are several recent publications on Raman characterization of SOI and sSOI substrates at a single excitation wavelength of choice [13-15]. By changing the wavelength of the illuminating signal, we obtain information from different depths. The probing depth of Raman measurements strongly depend on the light absorption properties of materials being examined at the excitation wavelength [16-19]. Since SOI and sSOI substrates are combined with a variety of Si top layer and buried oxide (BOX) thicknesses, the excitation wavelength should be chosen carefully. Unlike bulk Si substrates, SOI and sSOI substrates always show distinctive color due to the structure originated interference fringes. Probing depths of a given excitation wavelength can vary significantly, depending on the structure of the SOI and sSOI substrates. Very high resolution, multi-wavelength Raman measurements are required to properly characterize SOI and sSOI substrates. For statistically meaningful characterization and monitoring of high quality crystalline semiconductor materials, very high spectral resolution, measurement repeatability and long term stability ($< 0.1\ cm^{-1}$) are required. Conventional monochromator-based, compact Raman systems with moving mechanical and optical components cannot provide the stringent performance required for semiconductor material characterization.

A polychromator-based, high resolution multi-wavelength micro-Raman spectroscopy system (MRS-300) has recently been developed by Yoo, et al. and various characterization applications on Si stress in flash memory devices, Si stress surrounded by Cu filled through silicon vias (TSVs) and $Si_{1-x}Ge_x$/Si have been reported [16-19]. Raman signals from Si are measured and intensity, shift in wavenumber (cm^{-1}), full-width-at-half-maximum (FWHM), and asymmetry of the measured Raman peaks, are extracted and

*Corresponding author:
Tel : +82 2 2220 1772
Fax: +82 2 2296 1179
E-mail: parkjgL@hanyang.ac.kr

interpreted as quality factors for determining crystallinity, strain, stress and defects. Non-destructive depth profiling capability has also been demonstrated by extracting Raman signals from different excitation wavelengths.

Experiments

We have applied multi-wavelength Raman spectroscopy to sSOI samples with different top Si layer and BOX layer thicknesses. The stress and crystallinity of sSOI were characterized from the shift and FWHM of Raman peaks. The structure of the samples was analyzed from normal incidence optical reflectance spectra. The thickness of the strained Si film and BOX film of sSOI on Si (100) estimated from the reflectance spectra was compared with cross-sectional transmission electron microscopy (X-TEM) images.

Two sSOI samples with different top Si layer and BOX layer thicknesses were prepared. The strain and stress of the top Si layer of the sSOI samples are expected to differ from other samples because of the differences in the top Si layer and BOX layer thicknesses. For comparison purposes, one commercially available SOI sample and one bare Si sample were added as references. Raman measurements were done on all four samples using the MRS-300 system under excitation from three different wavelengths (457.9, 488.0, and 514.5 nm) from an Ar^+ laser [16-19]. Additional Raman measurements were taken from all four samples using a separate UV Raman system under 363.8 nm excitation for surface (shallow penetration of ~ 5 nm from the surface) characterization and comparison with the visible wavelength Raman results (with much deeper penetration).

Results and Discussion

Figs. 1(a) ~ (c) show normalized Raman spectra from a bare Si reference sample (A), an SOI sample (B), and two sSOI samples (C and D) under four different excitation wavelengths, along with relative probing depths of the various excitation wavelengths in a bulk Si sample and samples with a BOX layer. The probing depth in the bulk Si sample was estimated from optical absorption coefficients of Si at the appropriate excitation wavelength. SOI and sSOI substrates always have distinctive color due to the interference of light at the boundaries of each layer. Interpretation of multi-wavelength Raman measurements can provide additional insights into the samples.

UV Raman spectra of two sSOI samples (C and D) are very different from the other samples. The nominal thicknesses of sSOI films of the samples C and D are 10 and 14 nm, respectively. The nominal thicknesses of the top Si films of sample B is 50 nm. Sample C, with the thinnest nominal sSOI film (10 nm), showed both a strained Si peak at 509.94 cm^{-1} and a small bulk Si

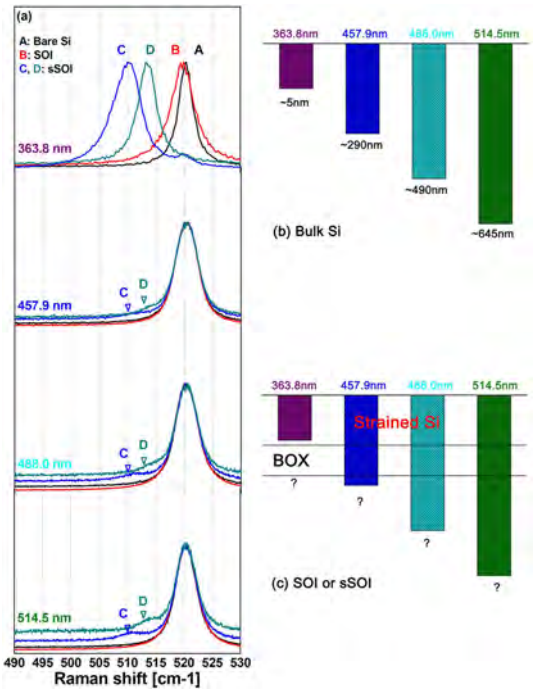

Fig. 1. Raman spectra (a) of four different samples, relative probing depths of various excitation wavelengths in (b) un-doped bulk Si and (c) SOI substrate.

peak from substrate at 520.30 cm^{-1}. Sample D, with the nominal sSOI film thickness of 14 nm, showed only one peak at 513.49 cm^{-1}. The SOI sample (B) and bare Si sample (A) showed one Raman peak at 519.75 and 520.30 cm^{-1}, respectively. The UV Raman spectra C and D clearly demonstrate the tensile strain increase with the decrease in the film thickness of sSOI. The tensile stress can be calculated from the magnitude of the Raman peak shift towards the lower wavenumber side (closer to) the stress free Si peak (520.30 cm^{-1}). One wavenumber (1 cm^{-1}), shift reduction, is equivalent to the increase in the tensile stress of 434 MPa [10, 12]. The estimated tensile stress of the samples C and D from UV Raman measurements, are 4.50 GPa and 2.96 GPa. The SOI sample (B) showed tensile stress of 673 MPa while the bare Si sample (A) was nearly stress-free.

All visible wavelength Raman spectra showed a very strong peak at 520.30 cm^{-1} due to the deeper probing depth of the excitation wavelengths. The thin sSOI samples C and D, which showed significant UV Raman peak shifts towards the lower wavenumber side (tensile strain), showed a small second peak at almost the same position as the UV Raman peak. It is quite interesting to see the small second peak from thin sSOI films increase its intensity with longer excitation wavelength (i.e. probing depth is getting deeper). It is the opposite phenomenon from our expectations from bulk Si measurement experience, as illustrated in Fig. 1(b). It can be interpreted as the effect of optical interferences between boundaries of the layered

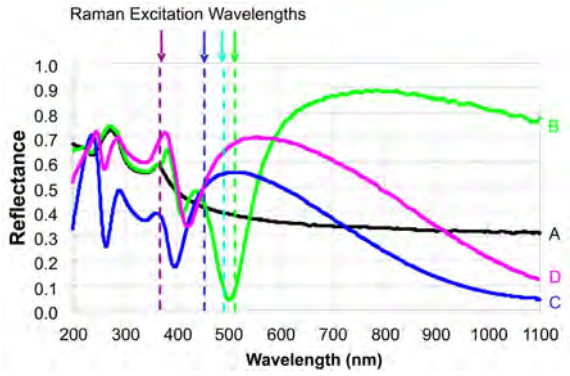

Fig. 2. Optical reflectance spectra of various samples in the wavelength range of 200 ~ 1100 nm with colored arrows indicating four Raman excitation wavelengths used in this study.

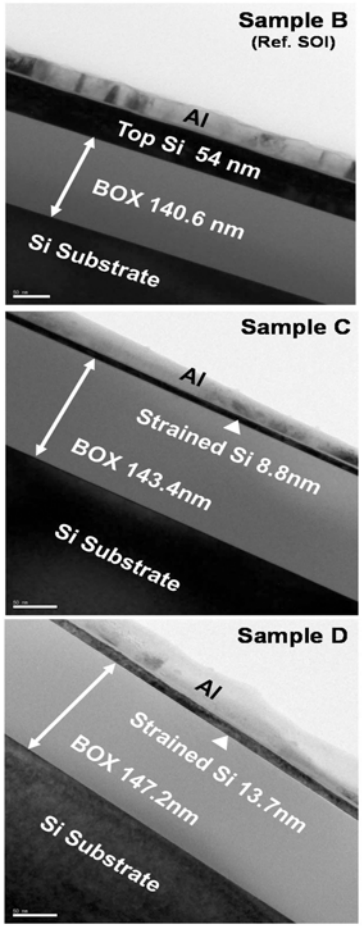

Fig. 3. Cross-sectional TEM images of silicon-on-insulator wafer (sample B) and two strained silicon-on-insulator wafers (sample C, D). All samples were capped with thin Al films for protecting the surface of sample and higher contrast images.

structures of the sSOI samples as illustrated in Fig. 1(c). When the sSOI layer is thicker than the penetration depth of the excitation wavelength, only one peak from the sSOI layer is observed under UV Raman measurement. Since the Raman signal provides weighted average information from the surface to the probing depth, observation of the substrate peak is very important for proper characterization of the sSOI layer. Multi-wavelength Raman characterization including a longer wavelength with a deeper probing (penetration) depth of intended sSOI film thickness adds an important dimension to the characterization. Figure 2 shows the normal incidence optical reflectance spectra from samples A ~ D in the wavelength range of 200 ~ 1100 nm. Four dotted vertical lines, at Raman excitation wavelengths, were added for easy comparison and proper interpretation of the Raman spectra measured at different excitation wavelengths. The thickness of the top Si layer and BOX layer of SOI and sSOI samples can be estimated by analyzing the reflectance spectra, assuming a $Si/SiO_2/Si$ multilayer model. The thicknesses of the Si film and the BOX layer estimated from the reflectance spectra, has been summarized in Table 1 with nominal thicknesses provided by SOI and sSOI manufacturers and physical thicknesses determined by X-TEM images. The Si stress values estimated by UV Raman spectra (of the top Si layers) were also summarized in the table.

The thickness estimated by optical reflectance spectra and X-TEM images are in reasonably good agreement with the nominal thickness values provided by the sample manufacturers, except for ultra-thin sSOI sample (C). The magnitude of error in thickness estimation using reflectance spectra tends to increase as film thickness becomes thinner. The error also increases when the sample structure becomes more complex due to the increase of the degrees of freedom. X-TEM images of two samples (C and D) with reference SOI (B) are shown in Fig. 3. Prior to X-TEM analysis, thin Al film was deposited on the samples for protecting the surface of sample and higher contrast images. X-TEM analysis can provide very vivid images of sample structure, but it is less practical because of its destructive nature and extensive sample preparation requirement. Furthermore, it only provides localized information due to the nature of its high magnification analysis. Stress or strain in thin Si film cannot be detected from X-TEM images unless micro-beam electron diffraction images are taken separately. The stress and strain of the sample can be relaxed during sample preparation.

Even though the thickness of thin sSOI samples estimated by the optical reflectance spectra may contain relatively large errors, it is still attractive as a non-destructive monitoring and quality control technique. Since the BOX layer thickness is generally thicker, and its variations are relatively small, it is possible to develop practical thickness estimation algorithms, with higher accuracy for SOI and sSOI samples, after getting enough cross-referenced data between reflectance spectra and X-TEM images. SiO_2/Si, SOI and sSOI samples have two common materials, SiO_2 and Si, however they behave substantially different from an optics point of view, depending on the thickness and stacking order. Interpretation of Raman spectra from multilayer samples, such as SOI and sSOI, must be

done carefully because the optical properties of the samples are significantly different, depending on structure, at a given wavelength as seen in Fig. 2.

These optical property differences have caused unexpectedly higher sensitivity of thin sSOI samples (samples C and D) at 514.5 nm excitation, with the deepest probing depth, in bulk Si. As seen in Fig. 2, the reflectance values of samples C and D are the highest at 514.5 nm compared to other visible excitation wavelengths. The majority of the probing light was reflected or rejected (i.e. only small portion of probing light actually penetrated into the sample, including the bulk Si). In other words, the effective penetration depths of 514.5 nm probing light in sSOI samples C and D might have been shallower than the other visible probing wavelengths of 457.9 and 488.0 nm.

UV Raman peaks from thin sSOI samples also show asymmetric shapes suggesting stress and strain in thin sSOI films are not uniform throughout the probing depths. The thin sSOI film (sample C) showed a broader peak than the thick sSOI film (sample D). The larger FWHM of UV Raman peak of sample C suggests the sSOI film has large strain, stress and crystallinity variation within the probing depth (~ 10 nm) compared to bare Si (A).

Conclusion

In conclusion, Multi-wavelength micro Raman and spectral reflectance measurement techniques have been applied to SOI and sSOI sample characterization and compared the results with X-TEM analysis results. We can conclude that the high resolution multi-wavelength Raman measurement, with spectral reflectance analysis, provide important insights for proper characterization of multilayer samples with nano-scale strained Si film.

Acknowledgments

This work was financially supported by the grant from the “Next-generation Substrate technology for high performance semiconductor devices (No. KI00 2083)” of the Ministry of Knowledge Economy (MKE) of Korea, the Brain Korea 21 Project in 2012 and the authors would like to thank Dr. Woo-Sik Yoo, Dr. Noriyuki Hasuike and Prof. Hiroshi Harima of Kyoto Institute of Technology for their experimental arrangement and very insightful discussions.

References

1. K. Rim, K. Chan, L. Shi, D. Boyd, J. Ott, N. Klymko, F. Cardone, L. Tai, S. Koester, M. Cobb, D. Canaperi, B. To, E. Duch, I. Babich, R. Carruthers, P. Saunders, G. Walker, Y. Zhang, M. Steen, M. Ieong, IEDM Tech. Dig. (2003) 49.
2. S.E. Thompson, S. Guangyu, C. Youn Sung, T. Nishida, IEEE Trans. Electron Devices. 53 [5] (2006) 1010.
3. Y.S. Lee, T.H. Shim, S.D. Yoo, J.G. Park, J. Appl. Phys. 103 [8] (2008) 084503.
4. Y. Haizhou, K.D. Hobart, R.L. Peterson, F.J. Kub, S.R. Shieh, T.S. Duffy, J.C. Sturm, IEDM Tech. Dig. (2003) 53.
5. W. Zhao, J.L. He, R.E. Belford, L.E. Wernersson, A. Seabaugh, IEEE Trans. Electron Devices. 51 [3] (2004) 317.
6. S.J. Kim, T.H. Shim, K.R. Choi, J.G. Park, Semicond. Sci. Technol. 24 [3] (2009) 035014.
7. T. Mizuno, N. Sugiyama, T. Tezuka, T. Numata, T. Maeda, S. Takagi, IEDM Tech. Dig. (2002) 31.
8. S. Takagi, J. Hoyt, J. Welser, J. Gibbons, J. Appl. Phys. 80 [3] (2009) 1567.
9. H. Harima, S. Nakashima, J.M. Carulli, C.P. Beetz, W.S. Yoo, Jpn. J. Appl. Phys. 36 (1997) 5525.
10. I. DeWolf, Semicond. Sci. Technol. 11 [2] (1996) 139.
11. H. Harima, J. Phys. Condens. Matter. 14 [38] (2002) R967.
12. I.D. Wolf, Spectroscopy Europe. 15 [2] (2003) 6.
13. A. Ogura, K. Yamasaki, D. Kosemura, S. Tanaka, I. Chiba, R. Shimidzu, Jpn. J. Appl. Phys. 45 (2006) 3007.
14. G. Taraschi, A.J. Pitera, L.M. McGill, Z.-Y. Cheng, M.L. Lee, T.A. Langdo, E.A. Fitzgerald, J. Electrochem. Soc. 151 [1] (2004) G47.
15. R.Z. Lei, W. Tsai, I. Aberg, T.B. O’Reilly, J.L. Hoyt, D.A. Antoniadis, H.I. Smith, A.J. Paul, M.L. Green, J. Li, R. Hull, Appl. Phys. Lett. 87 [25] (2005) 251926.
16. W.S. Yoo, K. Kang, T. Ueda, T. Ishigaki, Appl. Phys. Express. 2 (2009) 116502.
17. W.S. Yoo, T. Ueda, K. Kang, Ext. Abstr. Int. Conf. on Solid State Devices and Materials. (2008) 376.
18. A.D. Trigg, L.H. Yu, C.K. Cheng, R. Kumar, D.L. Kwong, T. Ueda, T. Ishigaki, K. Kang, W.S. Yoo, Appl. Phys. Express. 3 (2010) 086601.
19. Y.F. Tzeng, S. Ku, S. Chang, C.M. Yang, C.S. Chern, J. Lin, N. Hasuike, H. Harima, T. Ueda, T. Ishigaki, K. Kang, W.S. Yoo, Appl. Phys. Express. 3 (2010) 106601.